Results Using Response-Tailored Design Waves in Simulations of Extreme Roll of Multi-Hull Ships

Laura K. Alford, *University of Michigan*

Armin W. Troesch, *University of Michigan*

Muhamed Saeed Khalid, *University of Michigan*

ABSTRACT

Random, response-tailored wave trains are created for use in numerical simulations. Random wave trains generated by a finite number of components are tailored to produce a specified, linear, large response by considering the statistical distribution of the response phases in the neighborhood of a typical maximum response. The statistical distribution is seen to be non-uniform. Using a non-uniform distribution for the random phases of the response, design wave elevations leading to extreme roll motion may be calculated using linear theory and used as input to nonlinear seakeeping codes. Examples of design wave predictions resulting in extreme roll are included for various multi-hull ships.

Keywords: *response-tailored waves, non-uniform phase distributions, extreme roll, multi-hull ships*

1. INTRODUCTION

To properly design a structure, the naval architect must know what said structure must withstand over the course of its lifetime. To determine this, the designer traditionally has inflicted certain extreme conditions on the structure and estimated its response to these conditions to be the design response. When using computer simulations, these extreme conditions are usually an extreme sea state characterized by statistical parameters such as significant wave height and peak period. In these randomly simulated storms, however, there is no guarantee that the storm will produce the most likely extreme response.

The need to generate a specific extreme response has led to simulations involving response-tailored design waves: waves formulated such that the extreme response in question occurs during the finite time of the simulation. Recent research into response-tailored design waves includes work by Adegeest (1999), Clauss (2004), and Alford (2005).

Alford's work focuses on creating conditions that result in extreme roll for use in capsize investigations for a box barge and a high-speed containership. The method constructs a response time series using linear superposition of sinusoidal waves with a *non-uniform* phase distribution. The non-uniform response phase distribution produces a large linear response at a specified time. The incident wave phases are known from the linear seakeeping analysis and the response phases so the incident wave train may be calculated. This paper applies the above procedure to several concept models of high speed, multi-hull ships.

2. BACKGROUND

Even with modern computing power, nonlinear seakeeping analyses are expensive to run. Simulating three hours of storm conditions may require days of real time computing resources. However, if the design conditions have been tailored to produce the design response it only becomes necessary to simulate a very short record as the design response is guaranteed to occur. In order to create the sea conditions that will produce a design response, consider the usual construction of a random wave train.

Assuming linearity, stationarity, and ergodicity of the ocean for a short period of time, one may represent the ocean surface at some point *(x,y)* as the summation of many component waves:

$$\zeta(t) = \sum_{j=1}^{N} a_j \cos\left(\omega_j t + \beta_j\right) \tag{1}$$

$\zeta(t)$	wave elevation
N	number of components
a_j	amplitude of jth component
ω_j	frequency of jth component
β_j	phase of jth component

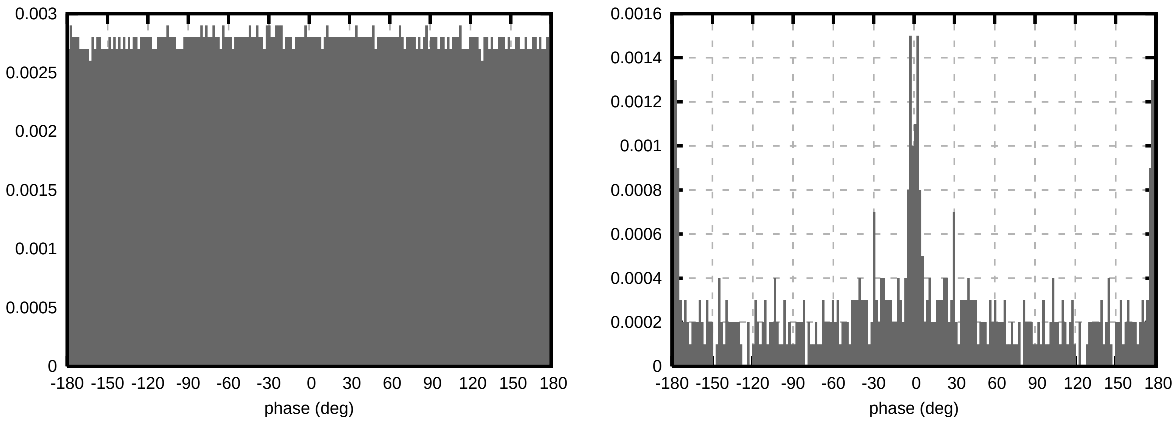

Figure 1 Phase distributions of two types of time series. *Left:* The combined phase distribution for 10 very long time series; T = 104,857.6 seconds, Δt = 0.1 seconds, N = 1,048,576 for each series. *Right:* The combined phase distribution for a short time series center about the maximum of each long time series; T = 1638.4 seconds, Δt = 0.1 seconds, N = 16384 for each time series.

The amplitudes and frequencies are determined by the spectrum (e.g. Pierson-Moskowitz, ITTC, Ochi 8-parameter, etc.) that will characterize the time series. The randomness enters through the phases, which are chosen from a uniform distribution between $-\pi$ and π. At each time step, the components are summed for the current *t* value and the wave elevation recorded. If this model is used to simulate many hours of exposure, eventually an extreme value will be recorded. Using the Fast Fourier Transform, any portion of the record may be broken down into its component amplitudes and phases. The number of components is determined by the time step and the length of the resulting time series.

$$N = T_{record} / \Delta t \tag{2}$$

The shorter record, being a subset of the longer, has the same time step, Δt, as the long record. Therefore, it is clear that as the record length decreases, so too does the number of available components. Figure 1 shows the difference between the phase distribution resulting from the very long simulation and the phase distribution resulting from a very short portion (~1.5%) of the simulation that is centered around a large extreme value.

When the long time record is considered, the phases are approximately uniformly distributed; in the limit of an infinite number of wave phases and a finite extreme value, the distribution is uniform. However, for the short time series that includes the extreme value there are fewer components available (Equation 2), and the phases become focused in order to achieve the same maximum.

The resulting phase distribution of the short time series depends on many factors including:

- the crest height, especially as relates to the RMS of the process (a measure of how extreme the event is)
- the number of components and, by Equation 2, the length of the short record

The relationship between the extreme value and the phase distribution that produced it is currently unknown, but it is clear that a non-uniform distribution must be used if short simulations are to be considered the equal of full-length storm simulations. Indeed, it may even be considered superior to the storm simulations as the non-uniform distribution ensures that the extreme value will occur within the finite simulation time.

3. METHOD: SOLVING THE INVERSE PROBLEM

The procedure for creating a response-tailored design wave train assumes that the wave train that elicits a large linear response is similar to the wave train that produces a large nonlinear response. Based on the above analysis of the phase distribution associated with an extreme wave amplitude, an extreme response may be generated by using the response spectrum with a non-uniform phase distribution. Once the response is known, the incident wave may be back-computed according to linear systems theory, and the result will be response-tailored waves suitable for investigating anything from a design midship bending moment to extreme roll. Solving for the incident wave, rather than the response, is known as the *inverse problem*.

The method used for this paper takes a simplified approach and assumes a zero-mean, Gaussian distribution with a given standard deviation for the response phases. In this paper, the response in question for all cases is roll.

The designer chooses a Target Extreme Value (TEV) of the response process to be produced. The TEV may be a function of many things, including: loading condition, heading angle, ship type, and sea state. Next, a linear seakeeping analysis is performed to calculate the 6 degrees of freedom (DOF) response amplitude operators (RAOs) of the ship and the RAO of the design response (if it is not one of the 6 DOF). The phases associated with the design response are then chosen according to a Gaussian distribution to ensure the extreme value chosen by the de-signer appears during the simulation, and the phases are then shifted so that the TEV occurs at the critical time. The phases for the incident wave are then back calculated via linear systems theory. Consider the representation of a linear system in Figure 2. Linear systems theory requires that the output have the same time dependence as the input, $e^{i\omega_j t}$, and due to the orthogonality property of Fourier Series the amplitude and phase of the output are:

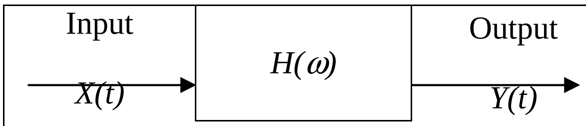

Process

Input $X(t) = x_j e^{i(\omega_j t + \beta_j)}$

Output $Y(t) = y_j e^{i(\omega_j t + \alpha_j)}$

RAO $H(\omega_j) = |H(\omega_j)| e^{i\gamma_j}$

Figure 2 Definition of the Variables in a Linear System.

$$y_j = \left| H(\omega_j) \right| x_j \tag{3}$$

$$\alpha_j = \gamma_j + \beta_j \tag{4}$$

Conversely, if one knows the response, *Y(t)*, and the linear function, *H(ω)*, the input may be calculated algebraically as:

$$x_j = \frac{y_j}{\left| H(\omega_j) \right|} \tag{5}$$

$$\beta_j = \alpha_j - \gamma_j \tag{6}$$

In this application, the input function is the incident wave, the linear function is the RAO of the response, and the output function is the design response. The relationships in Equations 5 and 6 hold for $j = 1, 2, \ldots, N$ because of the properties of superposition and orthogonality in linear systems. With the incident wave now known to produce an extreme linear response, linear and nonlinear responses may be calculated and compared.

4. LINEAR ANALYSIS AND NONLINEAR TIME SIMULATION OF BLENDED NONLINEAR HYDRODYNAMIC FORCES ON MULTI-HULL SHIPS

The geometry of multi-hull ships increases the difficulty of not only nonlinear time simulations but even the linear, frequency domain calculations. Extensive modifications were made to an existing linear seakeeping code for monohulls in order to properly capture the geometry of a multi-hull ship and include the effects of forward speed.

For the nonlinear time domain simulation, the total dynamic and static pressure field acting on an arbitrary body floating in water is evaluated. The displacements and other kinematics such as the relative velocities, accelerations, etc., and the structural loads in terms of dynamic shear forces, bending and torsion moments, etc. are calculated using direct integration of the pressures resulting from large motions of a multi-hull ship in six degrees of freedom. The method employs quasi-nonlinear radiation and diffraction models, and body exact hydrostatic and Froude-Krylov pressures. Nonlinear time simulation of large motions with exact Euler angles, shear forces and moments for regular waves and random seas are calculated for six degrees of freedom. Corresponding to the instantaneous position of the body, the quasi-nonlinear radiation and diffraction pressures are obtained through two and three dimensional radial basis functions. The frequency dependent components of the pressures are then Fourier transformed into the time do-main to obtain blended time dependent nonlin-ear pressures conforming to the instantaneous position of the arbitrary shape of the body; the instantaneous position appropriately includes the partially or fully submerged top deck for calculating the blended nonlinear pressures and forces.

The nonlinearities come from Euler angles, large motions, and the exact instantaneous intersection of the body and free surface. The free surface is obtained by superimposing incident gravity waves and the radiated and diffracted waves. Forward speed end corrections are calculated by converting the two dimensional velocity potential into a three dimensional mathematical function via radial basis function then partial differentiation is performed with respect to the longitudinal direction. In order to restore the two dimensional characteristics of the boundary value solution, a backward conversion to two dimensions is done to obtain a two dimensional mathematical function for the combined quasi-nonlinear nodal radiation and diffracted pressures. For the given instantaneous position of the node, the established mathematical function will produce the quasi-nonlinear value of the combined radiation and diffraction pressure by keeping track of the relative position of the other nodes on the two dimensional segment/station. Comprehensive validation studies are currently underway for this nonlinear time simulator.

Table 1 Ship particulars

Particulars	Catamaram		Compact Trimaram			Extended Length Trimaram		
	Overall Ship	**Demi-hulls**	**Overall Ship**	**Side Hulls**	**Center Hull**	**Overall Ship**	**Side Hulls**	**Center Hull**
LOA (m)	179	154	165.5	154	154	231	154	154
LWL (m)	154	154	154	154	154	231	154	154
B (molded, m)	32	11.2	55	10	10	55	10	10
Draft (m)	6.7	6.7	5	5	5	5	5	5
Displacement (t)	12,350	6175	12,350	4117	4115	12,350	4117	4115
Wet deck height (m)	11		9			9		
CL to CL (m)	20.8		22.5			22.5		
Vk (kts)	43		43			43		

5. RESULTS

The procedure described above has been used to create wave trains designed to induce extreme roll in three high speed, multi-hull ships: a catamaran, a compact trimaran, and an extended length trimaran. The hulls used to create all three ships are similar in length (see Table 1 for ship particulars) and differ in displacement such that each overall ship has the same displacement. The compact trimaran is essentially a catamaran hull in which a center hull has been added; in other words, the three hulls are placed "side-by-side-by-side". For an interesting comparison, the extended length trimaran was created by moving the center hull of the compact trimaran forward by L/2.

The exercise presented in this paper compares wave trains that produce a TEV of $4.5\sigma_{roll}$ and $5.5\sigma_{roll}$ for each hull in ITTC Sea State 7 ($h_{1/3}$ = 7.5 meters, T_p = 15.0 seconds). Here, σ_{roll} is the root-mean-square (RMS) of the roll process in Sea State 7. These TEVs have a probability of occurring of 1:25,000 and 1:3,700,000 respectively assuming a Rayleigh distribution for the peaks of the response. The actual value of the TEVs depends upon the heading angle. To determine the most severe roll cases given the Sea State 7 conditions, polar plots of the roll RMS were constructed for each ship. The heading angle chosen for the time simulations was that which produced the highest σ_{roll}. Therefore, while each extreme roll response that corresponds to a $4.5\sigma_{roll}$ or a $5.5\sigma_{roll}$ response has the same *probability*, it does not have the same *value*. This is just one choice of the Target Extreme Value needed in the procedure described above. The time simulations are 100 seconds long with the extreme response occurring at 50 seconds and use 201 non-zero wave components.

5.1 Catamaran

The roll polar plot for the catamaran is shown in Figure 3. The polar plot shows that the largest σ_{roll} occurs at a heading angle of 100° and has a value of 6.49°. Using this heading angle, the simulations in Figures 4 and 5 were created.

In both cases, the catamaran experiences a duration of enhanced roll both before and after the extreme roll event at *t = 50.0*. This duration seems to be about 25 seconds before and after the extreme event for the $4.5\sigma_{roll}$ case. For the $5.5\sigma_{roll}$ case, the duration before the extreme event is still around 25 seconds, but drops off to approximately 15 seconds afterwards. As for the wave train, it appears that a large roll angle for this catamaran is produced primarily by the slope of a single, large wave. Note that the wave height near the time of maximum roll was $2.1h_{1/3}$ and $2.5h_{1/3}$ for the $4.5\sigma_{roll}$ and $5.5\sigma_{roll}$ responses, respectively.

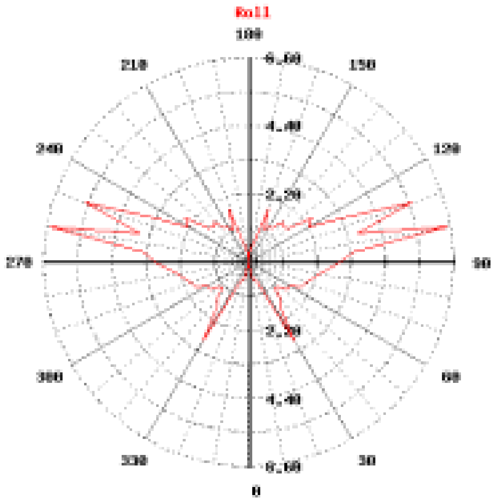

Figure 3 Symmetrical Catamaran: Polar plot - Roll RMS. ITTC Sea State 7. Forward speed = 43 kts.

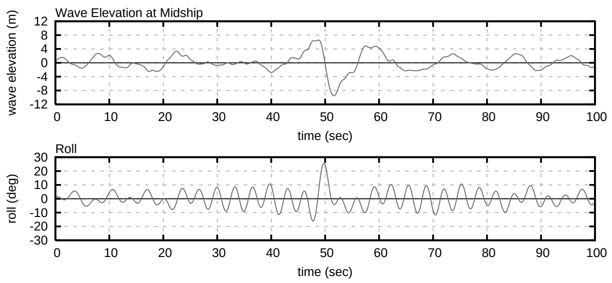

Figure 4 Symmetrical Catamaran: Design wave train leading to extreme roll of $4.5\sigma_{roll}$ = 29.2°. ITTC Sea State 7. Heading angle = 100°, forward speed = 43 kts.

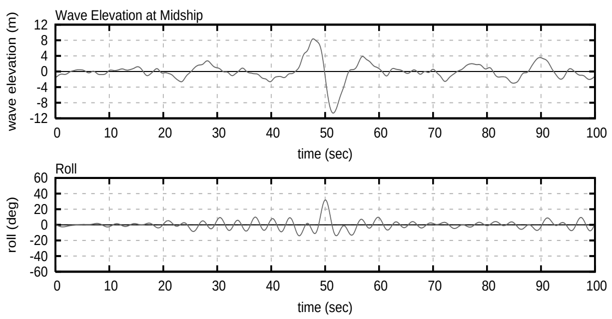

Figure 5 Symmetrical Catamaran: Design wave train leading to extreme roll of $5.5\sigma_{roll}$ = 35.7°. ITTC Sea State 7. Heading angle = 100°, forward speed = 43 kts

5.2 Compact Trimaran

The roll polar plot for the compact trimaran is shown in Figure 6. The polar plot shows that the largest σ_{roll} occurs at a heading angle of 95° and has a value of 1.46°. Using this heading angle, the simulations in Figures 7 and 8 were created.

There are several marked differences between the roll responses of the compact trimaran and of the catamaran. First, the compact trimaran does not experience any interval of enhanced roll. Rather, the extreme event, in both the $4.5\sigma_{roll}$ and $5.5\sigma_{roll}$ cases, appears rather alone with slightly deeper than average troughs preceding and following the event. The wave trains, however, do not show a particularly large wave to be the cause of extreme roll. Note that the wave height near the time of maximum roll was $1.3h_{1/3}$ and $2.1h_{1/3}$ for the $4.5\sigma_{roll}$ and $5.5\sigma_{roll}$ responses, respectively.

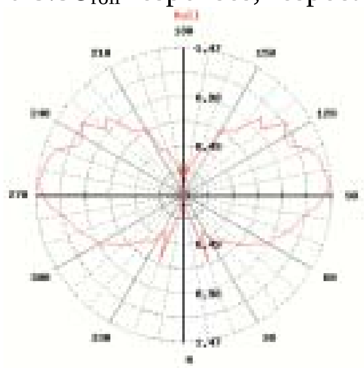

Figure 6 Compact Trimaran: Polar plot - Roll RMS. ITTC Sea State 7. Forward speed = 43 kts.

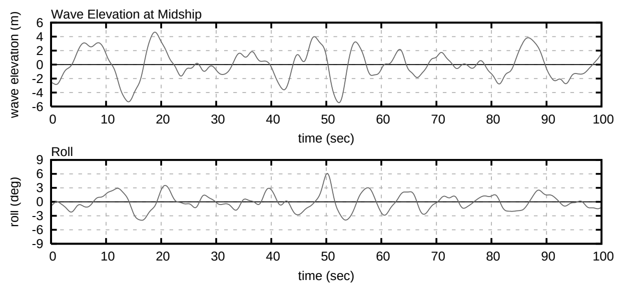

Figure 7 Compact Trimaran: Design wave train leading to extreme roll of $4.5\sigma_{roll}$ = 6.57°. ITTC Sea State 7. Heading angle = 95°, forward speed = 43 kts.

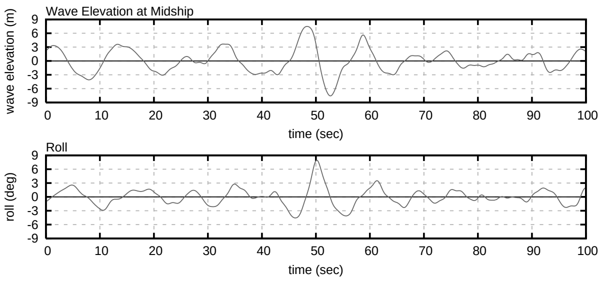

Figure 8 Compact Trimaran: Design wave train leading to extreme roll of 5.5σroll = 8.03°. ITTC Sea State 7. Heading angle = 95°, forward speed = 43 kts.

5.3 Extended Length Trimaran

The roll polar plot for the extended length trimaran is shown in Figure 9. The polar plot shows that the largest σ_{roll} occurs at a heading angle of 105° and has a value of 4.41°. Using this heading angle, the simulations in Figures 10 and 11 were created.

With the extended length trimaran, there is a return of the interval of enhanced rolling before and after the extreme events. This may be due to its resemblance in its aft sections to the catamaran. However, the duration of enhanced rolling after the extreme event appears much longer than seen above with the catamaran. The design wave trains include large, single waves, similar to those for the catamaran although not as large, suggesting that the extended length trimaran behaves similarly to the catamaran in roll. Note that the wave height near the time of maximum roll was $2.0h_{1/3}$ and $2.8h_{1/3}$ for the $4.5\sigma_{roll}$ and $5.5\sigma_{roll}$ responses, respectively.

6. CONCLUSIONS

The method just presented is a fast, efficient way to predict a design wave elevation leading to extreme responses from linear theory. As ship hulls become more and more complicated it becomes increasingly important to

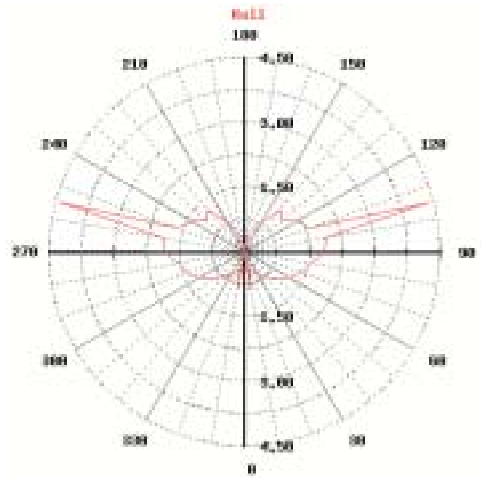

Figure 9 Extended Length Trimaran: Polar plot - Roll RMS. ITTC Sea State 7. Forward speed = 43 kts.

accurately predict extreme responses of these ships. Nonlinear seakeeping programs play a vital role in assessing the dynamic stability of these new hulls, but without a way to channel their resources the stability analyses are too expensive. The procedure and examples presented here show one way to efficiently use linear and nonlinear codes to evaluate new hulls. The procedure is especially helpful in the early design stages, where several hulls may be in contention. Potential instabilities may be exposed and efforts then concentrated on those designs showing more promise.

Ongoing research includes determining the relationship between the PDF of the phases around a maximum or minimum and possible input parameters. Also of interest is the probability of these design-tailored waves actually occurring in the real world. The designer needs to be able to assign a probability to each design wave or wave group that is calculated and assure it is physically realizable.

7. ACKNOWLEDGEMENTS

The work in this paper was partially supported by the National Defense Science and Engineering Graduate Fellowship; the Office of Naval Research (ONR)-NNRNE Program for Design Loads Generators; the ONR Tools for Multi-Hull Design Optimization Program; the ONR High-Speed SeaLift Project; and the Department of Naval Architecture and Marine Engineering, University of Michigan.

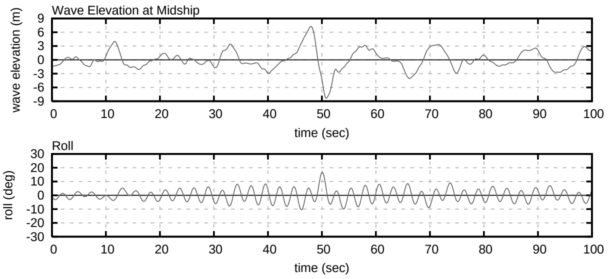

Figure 10 Extended Length Trimaran: Design wave train leading to extreme roll of $4.5\sigma_{roll}$ = 19.8°. ITTC Sea State 7. Heading angle = 105°, forward speed = 43 kts.

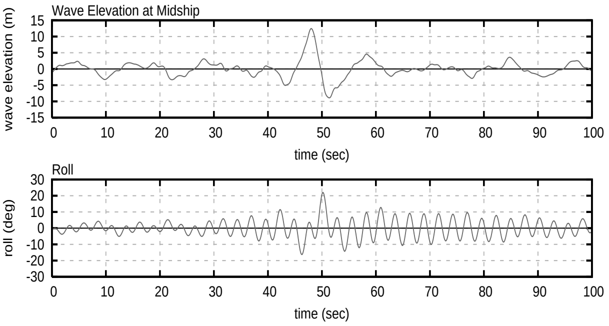

Figure 11 Extended Length Trimaran: Design wave train leading to extreme roll of $5.5\sigma_{roll}$ = 24.3°. ITTC Sea State 7. Heading angle = 105°, forward speed = 43 kts.

8. REFERENCES

Adegeest, L., Braathen, A., and Løseth, R. M., 1998, "Use of non-linear sea-loads simulations in design of ships," Proc. Practical Design of Ships and Mobile Units (PRADS), pages 53-58.

Adegeest, L., Braathen, A., and Vada, T., 1999, "Evaluation of methods for estimation of extreme nonlinear ship responses based on numerical simulations and model tests," Proc. Twenty-Second Symposium on Naval Hydrodynamics, pages 84-99.

Beck, R. F., and Troesch, A. W., 1990, Students documentation and users manual for the computer program SHIPMO.BM. Department of Naval Architecture and Marine Engineering, University of Michigan, Ann Arbor.

Chakrabarti, S., and Libby, A., 1988, "Further verification of gaussian wave packets," Applied Ocean Research, 10(2):106-108.

Clauss, G. F., 2002, "Task-related rogue waves embedded in extreme seas," Proc. Twenty-First International Conference on Offshore Mechanics and Arctic Engineering.

Clauss, G. F., and Bergmann, J., 1986, "Gaussian wave packets - a new approach to seakeeping tests of ocean structures," Applied Ocean Research, 10(2):190-206.

Clauss, G. F., and Hennig, J., 2003, "Deterministic analysis of extreme roll motions using tailored wave sequences," Proc. Eighth International Conference on the Stability of Ships and Ocean Vehicles, pages 441-455.

Clauss, G. F., and Hennig, J., and Schmittner, C. E., 2005, "Modelling extreme wave sequences for the hydrodynamic analysis of ships and offshore structures," Proc. Practical Design of Ships and Mobile Units (PRADS).

Clauss, G. F., and Hennig, J., and Schmittner, C. E., and Kühnlein, W. L., 2004, "Non-linear calculation of tailored wave trains for experimental investigations of extreme structure behaviour," Proc. Twenty-Third International Conference on Offshore Mechanics and Arctic Engineering.

Clauss, G. F., and Kühnlein, W. L., 1997, "Simulation of design storm wave conditions with tailored wave groups," Proc. First International Offshore and Polar Engineering Conference, pages 228-237.

Clauss, G. F., and Steinhagen, U., 1999, "Numerical simulation of nonlinear transient waves and its validation by laboratory data," Proc. First International Offshore and Polar Engineering Conference, pages 368-375.

Davis, M., and Zarnick, E., 1964, "Testing ship models in transient waves," Proc. Fifth Symposium on Naval Hydrodynamics, pages 507-543.

Jensen, J. J., and Pedersen, P. T., 2006, "Critical wave episodes for assessment of parametric roll," Proc. Ninth International Marine Design Conference, pages 399-411.

Jensen, J. J., 2005, "Conditional second-order short-crested water waves applied to extreme wave episodes," Proc. Ninth International Marine Design Conference, pages 399-411.

Pastoor, L. W., 2002, *On the Assessment of Nonlinear ship motions and loads*. PhD thesis, Technische Universiteit Delft.

Steinhagen, U., 2002, *Synthesizing Nonlinear Transient Gravity Waves in Random Seas*. PhD thesis, Technische Universität Berlin.

Takezawa, S., and Hirayama, T., 1976, "Advanced experimental techniques for testing ship models in transient water waves. Part II: The controlled transient water waves for using in ship motion tests," Proc. Eleventh Symposium on Naval Hydrodynamics, pages 37-54.

Takezawa, S., and Takekawa, M., 1976, "Advanced experimental techniques for testing ship models in transient water waves. Part I: The transient test technique on ship motions in waves," Proc. Eleventh Symposium on Naval Hydrodynamics, pages 23-35.

Taylor, P. H., Jonathan, P., and Harland, L. A., 1995, "Time domain simulation of jack-up dynamics with the extremes of a gaussian process," Offshore Technology, 1-A:53-58.

Tromans, P. S., Anaturk, A. R., and Hagemeijer, P., 1991, "A new model for the kinematics of large ocean waves - application as a design wave," Proc. First International Offshore and Polar Engineering Conference, pages 64-71.